Title

Ameloblastin is a cell adhesion molecule required for maintaining the differentiation state of ameloblasts

Journal

Journal of Cell Biology, 167(5)

ISSN

0021-9525

Authors

Fukumoto, Satoshi
Kiba, Takayoshi
Hall, Bradford
et al.

Publication Date

2004-12-06

DOI

10.1083/jcb.200409077

Peer reviewed

Ameloblastin is a cell adhesion molecule required for maintaining the differentiation state of ameloblasts

Satoshi Fukumoto,[1,2] Takayoshi Kiba,[1] Bradford Hall,[1] Noriyuki Iehara,[1] Takashi Nakamura,[1] Glenn Longenecker,[1] Paul H. Krebsbach,[3] Antonio Nanci,[4] Ashok B. Kulkarni,[1] and Yoshihiko Yamada[1]

[1]Craniofacial Developmental Biology and Regeneration Branch, National Institute of Dental and Craniofacial Research, National Institutes of Health, Bethesda, MD 20892
[2]Section of Pediatric Dentistry, Division of Oral Health, Growth and Development, Faculty of Dental Science, Kyushu University, Fukuoka 812-8582, Japan
[3]Department of Oral Medicine, Pathology and Oncology, School of Dentistry, The University of Michigan, Ann Arbor, MI 48109
[4]Department of Stomatology, Faculty of Dentistry, Université de Montréal, Montreal, QC, Canada H3C 3J7

Tooth morphogenesis results from reciprocal interactions between oral epithelium and ectomesenchyme culminating in the formation of mineralized tissues, enamel, and dentin. During this process, epithelial cells differentiate into enamel-secreting ameloblasts. Ameloblastin, an enamel matrix protein, is expressed by differentiating ameloblasts. Here, we report the creation of ameloblastin-null mice, which developed severe enamel hypoplasia. In mutant tooth, the dental epithelium differentiated into enamel-secreting ameloblasts, but the cells were detached from the matrix and subsequently lost cell polarity, resumed proliferation, and formed multicell layers. Expression of Msx2, p27, and p75 were deregulated in mutant ameloblasts, the phenotypes of which were reversed to undifferentiated epithelium. We found that recombinant ameloblastin adhered specifically to ameloblasts and inhibited cell proliferation. The mutant mice developed an odontogenic tumor of dental epithelium origin. Thus, ameloblastin is a cell adhesion molecule essential for amelogenesis, and it plays a role in maintaining the differentiation state of secretory stage ameloblasts by binding to ameloblasts and inhibiting proliferation.

Introduction

Many vertebral organs begin their development by inductive interactions between epithelium and mesenchyme. Tooth development is a classic example of this process and provides a useful experimental system for understanding the molecular mechanisms of organogenesis (Thesleff and Sharpe, 1997; Jernvall et al., 2000). The earliest morphogenetic event of mouse tooth development occurs at embryonic day (E) 11.5 when the oral ectoderm invaginates into the underlying neural crest-derived mesenchyme (Cohn, 1957). Continuation of this invagination results in the formation of epithelial tooth buds at E13.5. Mesenchymal cells surrounding the bud form the dental papilla, which later develop into dentin-secreting odontoblasts and the tooth pulp. After the bud stage, the tooth germ progresses to the cap and bell stages and the epithelium differentiates into enamel-secreting ameloblasts.

Ameloblasts undergo several differentiation processes (Fincham et al., 1999): the presecretory, secretory, and maturation stages. All these differentiation stages can be seen simultaneously in incisors of adult rodents because they continuously grow and erupt throughout life. In the presecretory stage, the basement membrane matrix separates the dental epithelium and mesenchymal preodontoblasts (Thesleff et al., 1981; Adams and Watt, 1993). However, the basement membrane matrix disappears at the secretory stage, and enamel matrix replaces the basement membrane to support and regulate the secretory ameloblast cells (Smith, 1998). The secretory stage ameloblasts produce and secrete specific proteins in the enamel matrix that are replaced by calcium and phosphorous during the maturation stage for enamel formation.

The principal components of the enamel matrix synthesized by secretory ameloblasts can be classified into two major categories: amelogenin, which makes up ~90% of the enamel matrix, and nonamelogenins including ameloblastin, enamelin, and tuftelin (Smith, 1998). Amelogenin-null mice (Gibson et al., 2001) exhibited a phenotype similar to human X-linked amelogenesis imperfecta in which ameloblast differentiation was normal but an abnormally thin enamel layer was formed. It has been suggested that amelogenins are essential for the organization of the crystal pattern and regulation of enamel thickness, and that other enamel proteins may play a role in the initial enamel formation and ameloblast differentiation (Fincham et al., 1999; Moradian-Oldak, 2001).

Ameloblastin, also known as amelin and sheathlin, is a tooth-specific glycoprotein, which represents the most abundant

The online version of this article contains supplemental material.

Correspondence to Yoshihiko Yamada: yoshi.yamada@nih.gov

Abbreviations used in this paper: E, embryonic day; ES, embryonic stem; P, postnatal day; SEM, scanning electron microscopic.

The Journal of Cell Biology, Vol. 167, No. 5, December 6, 2004 973–983
http://www.jcb.org/cgi/doi/10.1083/jcb.200409077

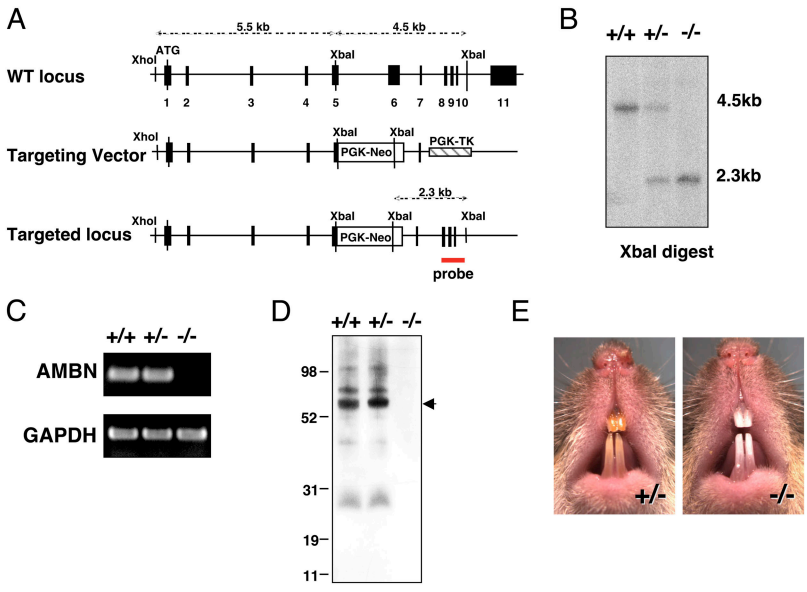

Figure 1. **Generation of ameloblastin-null mice.** (A) Structure of the *Ambn* gene, targeting vector, and targeted allele after homologous recombination. The location of the fragment used as a probe in Southern blotting is shown, as well as the sizes of the XbaI fragment detected for wild-type and targeted alleles. Exons are depicted as closed boxes. The PGK-neo and PGK-TK cassettes are depicted as open and oblique boxes. (B) Southern blot analysis of 6-wk-old mouse genomic DNA. Genomic DNA isolated from tails was digested with XbaI and hybridized with the probe containing exons 8–10. The wild-type and mutant alleles were detected as 4.5- and 2.3-kb fragments, respectively. (C) RT-PCR analysis of *Ambn* mRNA expression in wild-type, heterozygous, and homozygous mice. 2 μg of total RNA isolated from P3 mouse molars were reverse transcribed and amplified with primers for *Ambn* and *GAPDH*. (D) Western blot analysis of ameloblastin in wild-type, heterozygous, and homozygous mice. Two P3 maxillary first molars were dissected and lysed with 100 μl of lysis buffer, and 20 μl were separated by SDS-PAGE and immunoblotted with polyclonal anti-ameloblastin antibodies. (E) Incisors of 8-wk-old heterozygous and homozygous mice.

nonamelogenin enamel matrix protein (Cerny et al., 1996; Fong et al., 1996; Krebsbach et al., 1996). High levels of ameloblastin expression occur at the secretory stage and its expression is diminished at the maturation stage. Ameloblastin is also transiently expressed in dentin matrix and Hertwig's root sheath epithelial cells (Fong et al., 1996; Bosshardt and Nanci, 1998; Simmons et al., 1998), but its role in dentin and cementum formation has not been established. Unlike amelogenin, ameloblastin localizes near the cell surface and not in the deep enamel matrix layer (Nanci et al., 1998). Recently it was reported that transgenic mice overexpressing ameloblastin in ameloblasts resemble amelogenesis imperfecta, suggesting the importance of ameloblastin in enamel formation (Paine et al., 2003).

Here, we have generated mice with a null mutation at the ameloblastin locus to determine the role of ameloblastin in amelogenesis. The mutant mice showed several specific anomalies of tooth development including the lack of enamel formation. In ameloblastin-null mice, the dental epithelium differentiates into enamel-secreting ameloblasts, but the cells detach from the matrix surface at the secretory stage and lose cell polarity. Mutant ameloblasts resume proliferation and accumulate to form multiple cell layers, producing abnormal, unstructured, calcified matrix. Ameloblastin binds specifically to ameloblasts and inhibits cell proliferation of mutant ameloblasts. In mutant teeth, ameloblasts regain some early phenotypes of undifferentiated dental epithelial cells, and the abnormalities occur when the cells detach. Our results indicate that ameloblastin is a key adhesion molecule for enamel formation and suggest that ameloblastin plays an important role by binding to, and maintaining the differentiated phenotype of secretory ameloblasts.

Results

Generation of ameloblastin-null mice

To analyze the function of ameloblastin, we performed targeted disruption of the ameloblastin gene (*Ambn*) in mouse embryonic stem (ES) cells using homologous recombination. We deleted the sequence containing exons 5 and 6 of the gene and replaced it with the PGK-Neo^r cassette gene (Fig. 1 A). Chimeric mice were produced from ES cell clones with the modified *Ambn* locus as confirmed by genotyping with Southern blotting (Fig. 1 B). Neither *Ambn* transcript nor protein was detected in postnatal day (P) 3 maxillary first molar of homozygous ($Ambn^{-/-}$) mice (Fig. 1, C and D). Heterozygous mice ($Ambn^{+/-}$) showed similar expression levels of ameloblastin as wild-type mice.

Defective enamel formation in ameloblastin-null mice

The *Ambn*-null mice were fertile, and the newborns appeared normal. However, as early as 3 wk old, incisors from $Ambn^{-/-}$ mice displayed a chalky white color, indicating hypoplastic or hypocalcified enamel (Fig. 1 E). Stereomicroscopic analysis of molars and incisors of 3-wk-old heterozygous mice showed translucent enamel, whereas $Ambn^{-/-}$ molars and incisors lacked enamel (unpublished data). Microradiographic imaging showed normal development of the craniofacial bone and the outward appearance of tooth (Fig. 2 A). It was reported that ameloblastin is transiently expressed in Hertwig's root sheath (Fong et al., 1996; Bosshardt and Nanci, 1998; Simmons et al., 1998). However, root formation in the mutant mice was not different from wild-type and $Ambn^{+/-}$ mice (unpublished data). Both maxillary and mandibular incisor tips of $Ambn^{-/-}$ mice were rounded, and the occlusal plane of the molar was flattened (arrow) because of attrition after tooth eruption (Fig. 2 B). Interestingly, the space between tooth and alveolar bone (arrows) was wider in $Ambn^{-/-}$ mice than in $Ambn^{+/-}$ mice. In this space, invasion of calcified tissue was observed (Fig. 2 B).

CT-scans of molars from 6-wk-old $Ambn^{+/-}$ mice showed that radio-opaque enamel formed over dentin, whereas in $Ambn^{-/-}$ teeth, there was no radio-opaque enamel region and the occlusal surface was flat (Fig. 2 C). Scanning electron microscopic (SEM) analysis of $Ambn^{-/-}$ incisors revealed a dys-

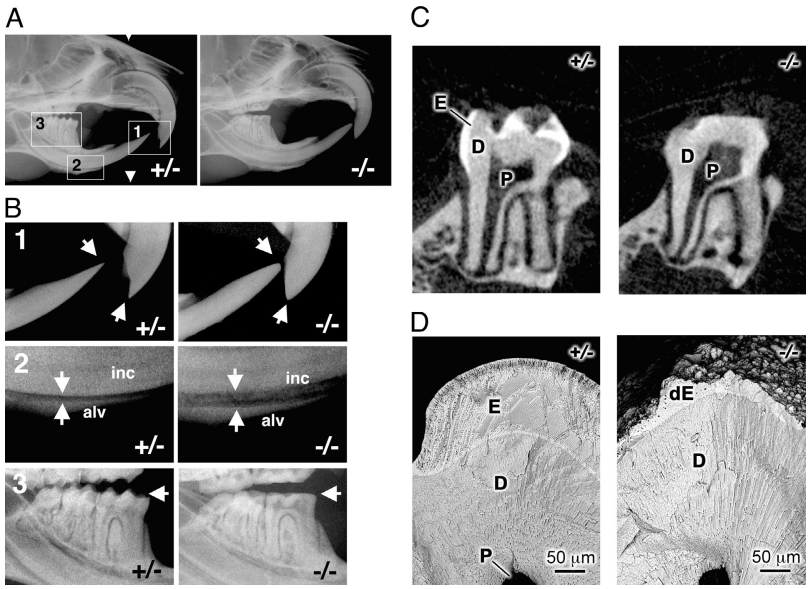

Figure 2. **Defects in enamel formation of ameloblastin-null mice.** (A) Faxitron analysis of the craniofacial region of 8-wk-old heterozygote and homozygote mice. Boxed areas were enlarged in B, 1–3. (B) High magnification of incisor tips (1), bottom incisors and alveolar bone space (2), and bottom molars (3). Round incisor tips, wider incisor-alveolar bone space, and a flat occlusal plane are observed in mutant mice. Arrows indicate incisor tips, incisor-alveolar bone space, and occlusal planes. inc, incisor; alv, alveolar bone. (C) CT-scan analysis of top first molar of heterozygous and homozygous mice. E, enamel; D, dentin; P, pulp. (D) SEM analysis of incisor. E, enamel; D, dentin; p, pulp, dE, defective enamel.

plastic layer with a rough surface over dentin and lack of a prism pattern, which is the hallmark of organized mineral crystals in normal enamel (Fig. 2 D).

Detachment of ameloblasts from the matrix and formation of multicell layers

In early molar development (E18), there were no differences in tooth size and shape between normal and *Ambn*$^{-/-}$ mice (Fig. 3 A). In P1 molars, dentin formation had begun and dental epithelium had started to elongate with the apical nuclear localization in both control and *Ambn*$^{-/-}$ mice. Thus, cellular organization of ameloblasts and odontoblasts was indistinguishable between normal and *Ambn*$^{-/-}$ mice at the presecretory stage. However, at P3, ameloblasts of *Ambn*$^{-/-}$ mice started to detach from the matrix layer and lose cell polarity seen as the centralized nuclear localization, whereas normal ameloblasts were polarized, elongated, and formed an enamel matrix (Fig. 3 A). At P7, *Ambn*$^{-/-}$ ameloblasts completely lost their polarity (short and round shape) and accumulated to form a multilayered structure, in contrast to the single layer of *Ambn*$^{+/-}$ ameloblasts. Similar to molars, cellular organization of presecretory stage ameloblasts of *Ambn*$^{-/-}$ incisors was normal (Fig. 3 B). At the early secretory stage, the mutant incisors have a zone where ameloblasts detach from the matrix and remain as a single cell layer. In the advanced stage, these cells lose polarity and form a multicell layer. In addition, connective tissues were formed underneath the detached ameloblast layer, which contained irregular calcified structures (Fig. 3 B, arrows). This calcified structure was confirmed by the presence of phosphocalcium in the energy dispersive analysis (unpublished data).

To determine the cell type of the multicell layer observed in *Ambn*$^{-/-}$ tooth, we immunostained tissue sections with antibodies to ameloblast marker proteins, which are expressed in normal secretory ameloblasts of P7 molars (Fig. 3 C). The multicell layer in *Ambn*$^{-/-}$ mice showed positive immunostaining for enamelin and tuftelin, whereas amelogenin was weak, but was present in the matrix globules (arrows). These results suggest that the multilayered cells are derived from ameloblasts. Accumulated ameloblasts in *Ambn*$^{-/-}$ mice were PCNA positive, indicating that they were proliferating (Fig. 3 D). In *Ambn*$^{+/-}$, ameloblasts were PCNA negative, indicating that at this secretory stage, ameloblasts stopped proliferating. These results indicated that ameloblasts in *Ambn*$^{-/-}$ mice lost cell polarity, changed their morphology, and proliferated at the secretory stage.

Expression analyses of regulatory factors and tooth matrix proteins

To better characterize and gain insight into the mechanism of the abnormalities of ameloblasts in mutant mice, we examined the expression of regulatory factors and tooth marker proteins (Figs. 4 and 5). It was shown that the homeobox-containing transcription factor Msx2 was expressed in undifferentiated ameloblasts but was down-regulated in secretory stage ameloblasts (Maas and Bei, 1997). P3 *Ambn*$^{+/-}$ ameloblasts expressed the Msx2 protein but its expression was diminished in P7 ameloblasts (Fig. 4). In mutant *Amb*$^{-/-}$ mice, Msx2 was expressed at P3 ameloblasts, similar to P3 *Ambn*$^{+/-}$ tooth. However, Msx2 was still expressed in a multiple cell layer of ameloblasts of P7 mutant tooth in contrast to P7 control tooth. p27, a Cdk inhibitor, was strongly expressed in P7 ameloblasts compared with P3 ameloblasts in *Ambn*$^{+/-}$ tooth (Bloch-Zupan et al., 1998), whereas its expression remained weak in P7 ameloblasts of mutant tooth. p75, a member of the TNF receptor family, was expressed in P3 *Ambn*$^{+/-}$ ameloblasts, and its expression was diminished at P7 (Mitsiadis et al., 1993). In contrast, p75 was expressed strongly in ameloblasts in P7 mutant tooth. Similar expression patterns of these proteins were observed in incisors containing all differentiation stages of the dental epithelium (unpublished data). Immunostaining of p27 was positive in immediate-early *Ambn*$^{-/-}$ ameloblasts, but it was reduced in the multicell layer of early secretory ameloblasts (unpublished data). This suggested that the proliferation of ameloblasts stopped at the im-

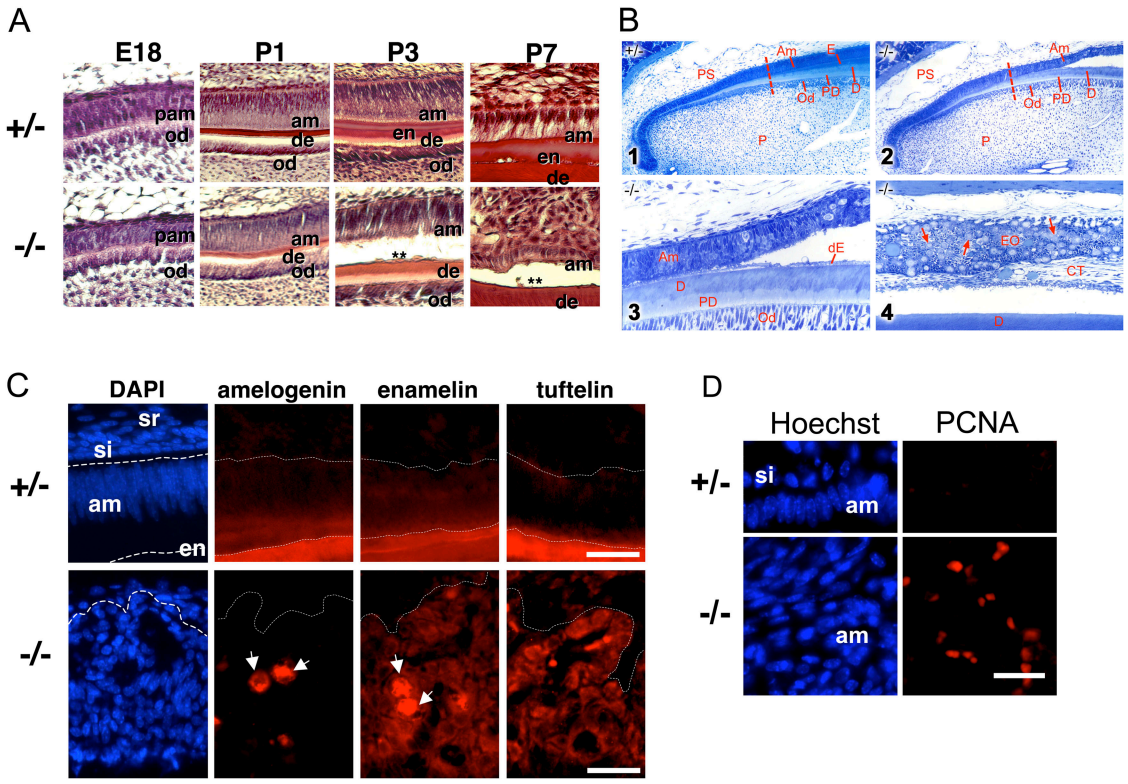

Figure 3. **Histology of molars and incisors and characterization of multilayered cells.** (A) Hematoxylin-eosin staining of top first molars of E18, P1, P3, and P7 heterozygous (top) and homozygous (bottom) mice. Loss of cell polarity and detachment from the matrix were observed in P3. P7 molar ameloblast cells accumulate and fail to form columnar shaped single cell layers. (B) Incisors in 6-wk-old heterozygous (1) and homozygous (2) mice. High magnifications of the presecretory and secretory stages (3) and the early maturation stage (4) of mutant incisors. *Ambn*$^{-/-}$ ameloblasts form multiple layers containing abnormal calcified structures (arrows). Connective tissue (CT) was migrated into the detached space between ameloblasts and the matrix surface. Am, ameloblasts; D, dentin: EO, enamel organ; Od, odontoblasts; PS, presecretory stage; PD, predentin; P, pulp; E, enamel layer; arrows, calcified structures, dE; defective enamel. (C) Immunostaining of P7 normal (top) and mutant molars (bottom) with anti-amelogenin, enamelin, and tuftelin antibodies and Cy-3-conjugated secondary antibody. DAPI staining was used for nuclear localization. Dashed lines show the border between ameloblasts and the stratum intermedium interface (top) and margin of multilayered cells (bottom). Arrows indicate abnormal matrix accumulating enamel matrix proteins. (D) PCNA immunostaining of ameloblasts (right) and nuclear staining with Hoechst dye (left). am, ameloblast; si, stratum intermedium; en, enamel; sr, stellate reticulum. Bars, 25 μm.

Figure 4. **Expression of Msx2, p27, and p75 in molar and incisor ameloblasts.** P3 and P7 molars and 6-wk-old incisors were fixed and decalcified. Paraffin sections were stained with DAPI for nuclear localization and immunostained with antibodies for Msx2, p27, and p75. (A) P3 and P7 molars of Ambn$^{+/-}$ and (EB) Ambn$^{-/-}$ mice. Msx2 was expressed in ameloblasts of both P3 and P7 Ambn$^{-/-}$ tooth, whereas it was expressed in P3 but not P7 Ambn$^{+/-}$ ameloblasts. p27 was expressed in P7 Ambn$^{+/-}$ ameloblasts but not P7 Ambn$^{-/-}$ ameloblasts, but p75 was expressed in P7 Ambn$^{-/-}$ ameloblasts but not in P7 Ambn$^{+/-}$ ameloblasts. sr, stellate reticulum; si, stratum intermedium; ab, ameloblast.

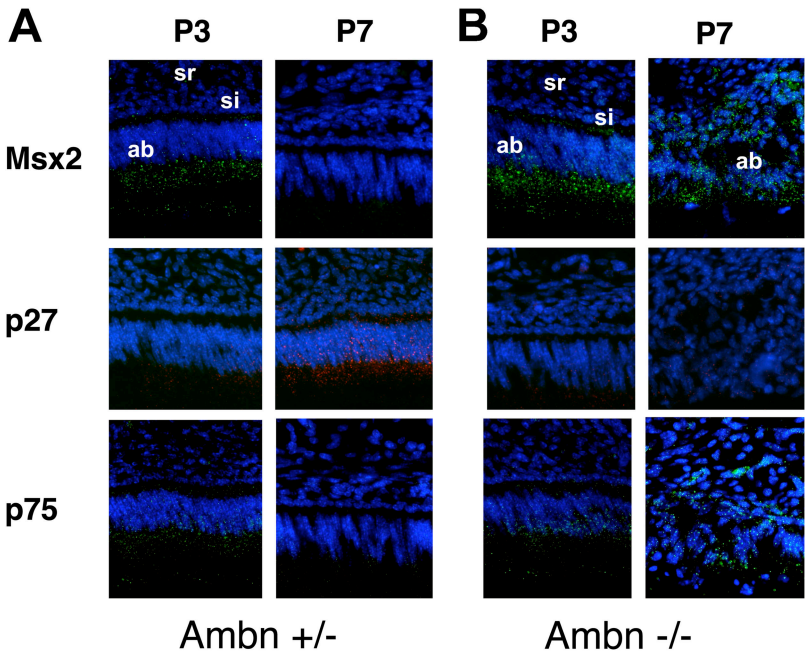

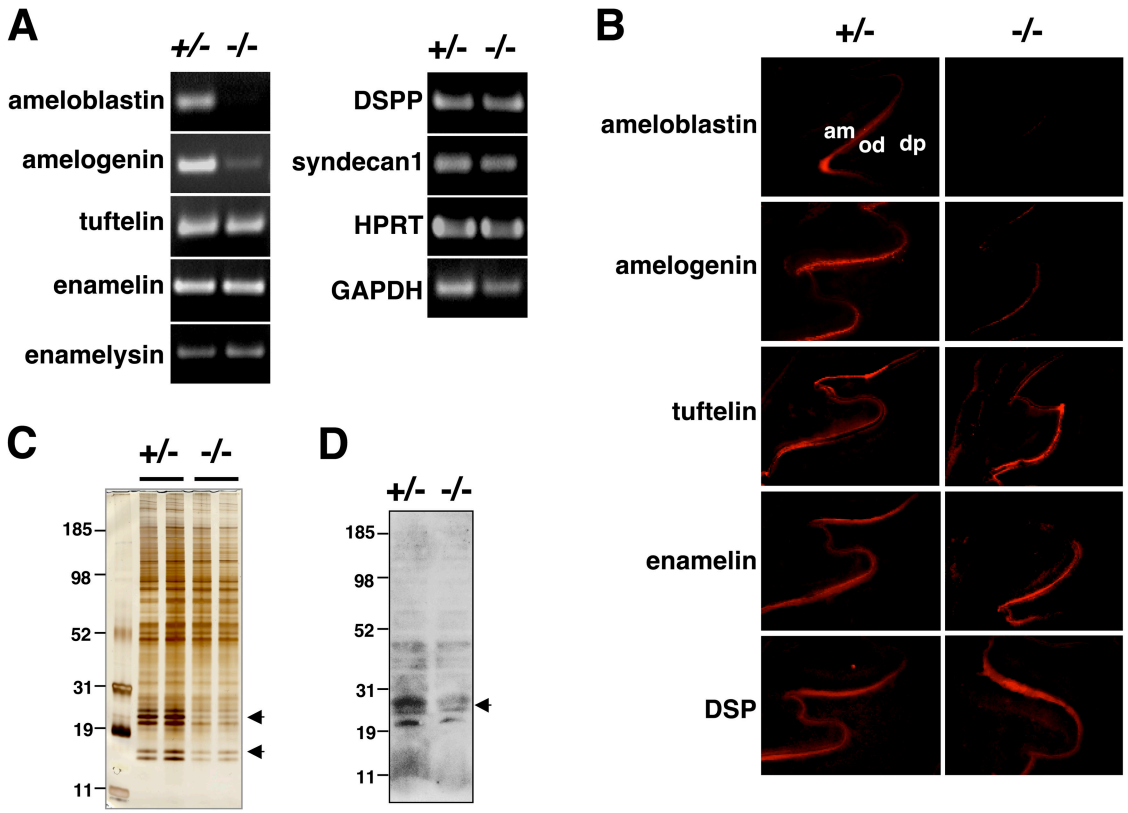

Figure 5. **Expression of tooth markers in mutant mice.** (A) mRNA expression in P3 mandibular first molars by RT-PCR. (B) Immunostaining of tooth marker proteins, ameloblastin, amelogenin, tuftelin, enamelin, and dentin sialoprotein (DSP) in P3 molars. There is no ameloblastin staining in mutant molars. (C) Silver staining of total lysates from P3 mandibular molars from two different heterozygous and mutant mice separated by SDS-PAGE. Arrows indicate the amelogenin protein and their cleaved derivatives. (D) Western blot analysis of amelogenin in P3 mandibular first molars.

mediate-early secretory stage but resumed from the early secretory stage. These results suggest that in mutant tooth, *Ambn*$^{-/-}$ ameloblasts regain certain early phenotypes of undifferentiated dental epithelium, when cells detach from the matrix and form a multicell layer.

RT-PCR analysis showed the absence of ameloblastin mRNA and significantly reduced amelogenin mRNA expression in P3 *Ambn*$^{-/-}$ molars (Fig. 5 A), but there were no differences in mRNA levels for enamelin, tuftelin, DSP, and enamelysin between normal and *Ambn*$^{-/-}$ molars. Amelogenin was immunostained weakly in P3 *Ambn*$^{-/-}$ molars compared with normal molars (Fig. 5 B). Other tooth proteins, including enamelin, tuftelin, dentin matrix protein DSP, and enamelysin, were expressed at similar levels to normal mice. We also confirmed the reduced expression of amelogenin proteins by SDS-PAGE and Western blotting (Fig. 5, C and D). These results suggest that dental epithelial cells of mutant mice differentiate into enamel matrix-secreting ameloblasts.

Change in ECM during ameloblast differentiation

The basement membrane provides a scaffolding for epithelium and signaling for cellular differentiation in many tissues through interactions of specific cellular receptors (Yurchenco and O'Rear, 1994; Timpl, 1996). Because secretory stage ameloblasts of *Ambn*$^{-/-}$ mice showed loss of cell polarity and abnormal proliferation with detachment from the matrix, we examined the basement membrane by immunostaining normal and *Ambn*$^{-/-}$ incisors (Fig. 6). In normal incisors, localization patterns of the basement membrane (stained for collagen IV and laminin β1/γ1 [subunits of laminin 10/11, a major laminin in early tooth development]) and enamel matrix (stained for ameloblastin) were reciprocal (Fig. 6). The basement membrane was present at the basal lamina underneath presecretory stage ameloblasts (preameloblasts), however, at the secretory stage they disappeared and the enamel matrix emerged with some overlapping in the intermediate stage (enamel layer indicated by dotted lines). Expression patterns of integrin α6, a receptor of laminin, are similar to that of the basement membrane: it was localized at the basal layer of preameloblasts, but disappeared when preameloblasts differentiated into ameloblasts. In mutant incisors, the expression patterns of the basement membrane and integrin α6 were similar to normal incisors. It was reported that laminin 5, epithelial laminin consisting of α3β3γ2, was synthesized by secretory stage ameloblasts (Salmivirta et al., 1997; Ryan et al., 1999). Weak expression of the laminin γ2 chain was observed at the early secretory stage, and its strong expression started at the late secretory stage and continued through the maturation stage, indicating that its expression is delayed compared with ameloblastin (Fig. 6). Significant staining of the laminin γ2 chain was observed in the basal cytoplasm part

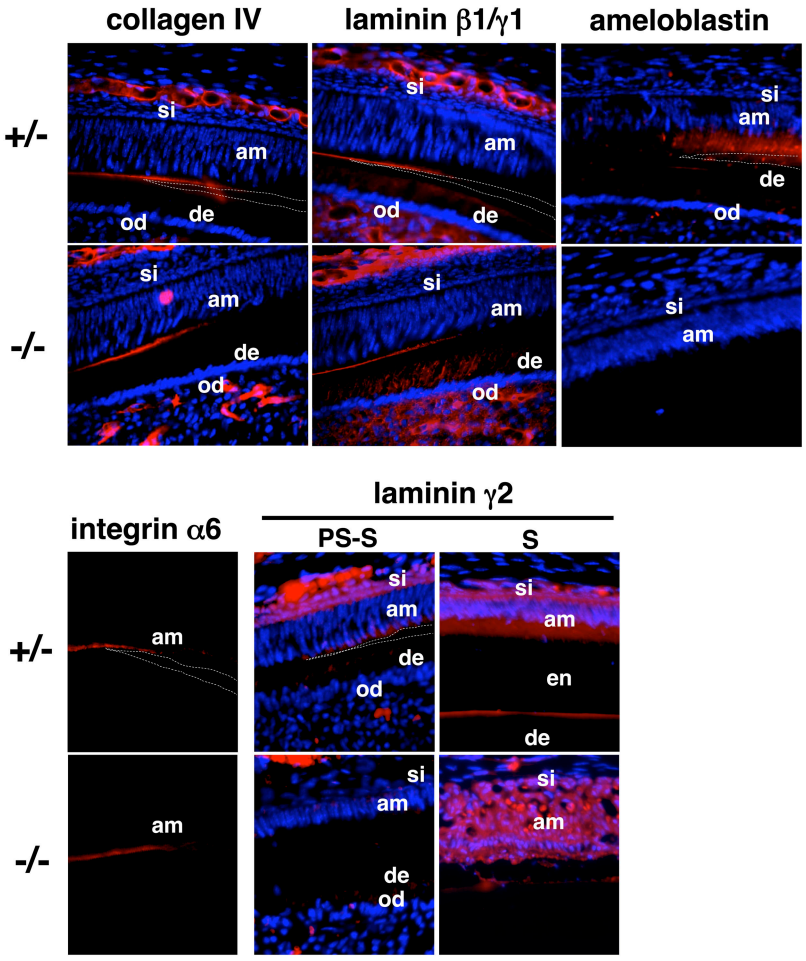

Figure 6. **Immunostaining of basement membrane and integrin in incisors.** 6-wk-old mouse maxillas were fixed and decalcified. Paraffin sections of incisors of heterozygous and mutant mice were immunostained with antibodies to amelogenin, collagen IV, laminin 1, integrin α6, and laminin γ2 and visualized with Cy-3-conjugated secondary antibody. Polyclonal antibodies to laminin 1 react with α1, β1, and γ1. Laminin α1 is not present and the tooth basement membrane contains laminin 10 (α5, β1, and γ1). am, ameloblast; si, stratum intermedium; od, odontoblast; en, enamel; de, dentin.

of late secretory ameloblasts. This localization pattern is different from that of laminin β1/γ1 immunostaining where most of the staining was found in the basal lamina. In the mutant, laminin γ2 was synthesized and deposited in the matrix surrounding abnormally accumulated ameloblasts. There is no difference in basement membrane formation between normal and mutant teeth at the presecretory stage. However, in a more advanced secretory stage, where ameloblastin is synthesized, abnormalities are obvious and progressive. Thus, ameloblastin is a candidate matrix protein for supporting secretory stage ameloblasts.

Cell type–specific binding of ameloblastin

Because ameloblasts detach from the matrix in the absence of ameloblastin, we hypothesized that ameloblastin may be involved in cell–matrix interactions.

We examined the binding of ameloblastin to cells. Recombinant His-tagged ameloblastin was produced in COS7 cells, purified by affinity chromatography and used for cell adhesion assays (Fig. 7). Dental epithelial cells from P3 molars adhered dishes coated with ameloblastin in a dose-dependent manner, whereas a control His-tagged protein showed no cell adhesion (Fig. 7 A). Cell binding activity of ameloblastin appears to be specific to dental epithelium because ameloblastin did not support cell adhesion to other cells including kidney epithelial cell line MDCK (Fig. 7 B). We next examined substrate-specific adhesion of ameloblasts from wild-type tooth (Table I). Because primary dental epithelial cells isolated from P7 molars contain mixed cell populations, we distinguished between preameloblast and ameloblast cell types that had adhered to substrates by immunostaining of integrin α6 and amelogenin. We found that ameloblasts (amelogenin positive and integrin α6 negative) adhered to ameloblastin, but not fibronectin

Table I. **Cell type–specific binding to ameloblastin**

	Immunostaining of bound cells (%)		
	Intα6(+) AMEL(−)	Intα6(+) AMEL(+)	Intα6(−) AMEL(+)
Substrate	**Preameloblasts**	**Intermediate**	**Ameloblasts**
None	N/A	N/A	N/A
rAMBN	2.4 ± 1.1	38.3 ± 5.6	52.8 ± 6.9
Fibronectin	70.6 ± 8.2	12.7 ± 3.8	3.1 ± 1.2
Laminin 10/11	62.1 ± 7.5	21.4 ± 5.2	5.8 ± 3.7

Dental epithelial cells from P3 normal molars were plated to dishes coated with ameloblastin (rAMBN), fibronectin, or laminin 10/11 at 10 μg/plate. Bound cells were double immunostained with antibodies to amelogenin (AMEL) and integrin α6 (Intα6). Numbers of immunostained cells are shown as percent of bound cells.
N/A, not applicable.

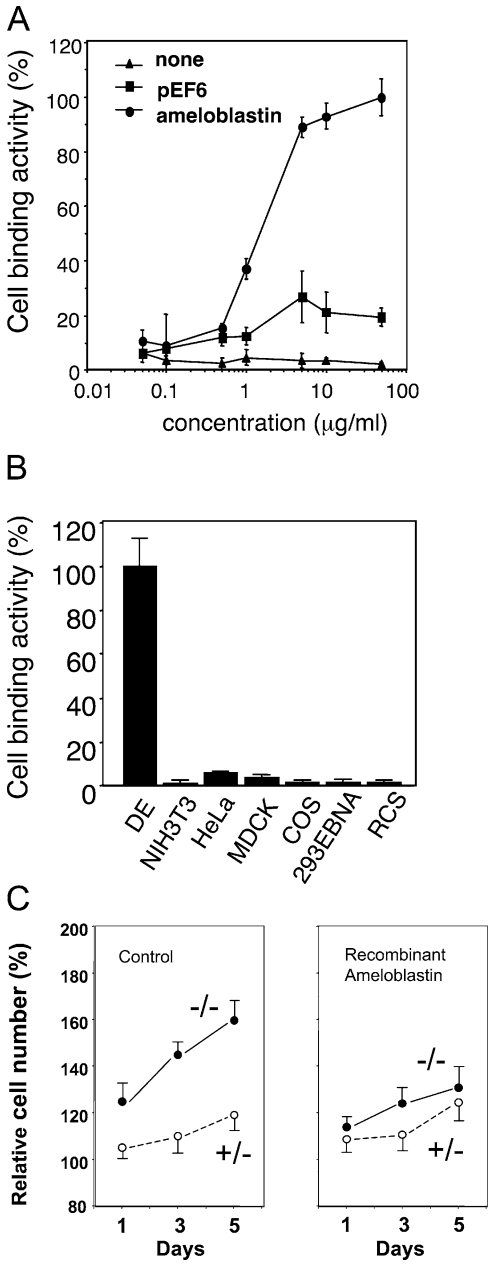

Figure 7. **Ameloblastin binds dental epithelium and inhibits proliferation of Ambn$^{-/-}$ ameloblasts.** (A) Adhesion of dental epithelial cells isolated from P3 molars to dishes coated with various amounts of recombinant ameloblastin. pEF6 is a control protein containing only the His-tagged portion purified from mock-transfected cells (pEF6, square). (B) Cell type–specific adhesion to recombinant ameloblastin. Various types of cells were plated on dishes coated with ameloblastin (10 μg/plate), and bound cells were counted. DE, dental epithelial cells. (C) Inhibition of ameloblast proliferation by maeloblastin. Dental epithelial cells from normal and mutant P7 molars were incubated on plates without (left) or with recombinant ameloblastin (right; 10 μg/plate). Plating cell numbers at day 0 are set as 100%. Proliferation of cells from P7 mutant mice are significantly inhibited by ameloblastin. Data are expressed as mean of triplicate results.

and laminin 10/11. In contrast, preameloblasts (integrin α6 positive and amelogenin negative) adhered to fibronectin and laminin 10/11, but not ameloblastin. Intermediate stage cells (positive for both amelogenin and integrin α6) adhered to all three substrates. These results suggest that ameloblasts but not preameloblasts preferentially adhered to ameloblastin.

Inhibitory activity of ameloblastin for proliferation of *Ambn*$^{-/-}$ ameloblasts

Because *Ambn*$^{-/-}$ ameloblasts proliferate and accumulate in a multicell layer at the secretory stage, we hypothesized that proliferation of these cells may be blocked by ameloblastin. We prepared P7 dental epithelial cells from normal and *Ambn*$^{-/-}$ teeth and measured their proliferation in the presence of recombinant ameloblastin (Fig. 7 C). In the absence of ameloblastin, control *Ambn*$^{+/-}$ cells showed slow proliferation with about a 20% increase in cell number in 5-d cultures, whereas cells from *Ambn*$^{-/-}$ tooth proliferated more rapidly, increasing by 75% in the same time period (Fig. 7 C, left). The majority of proliferating *Ambn*$^{-/-}$ cells are amelogenin positive, indicating ameloblasts (unpublished data). The ability to proliferate in culture is consistent with that of accumulated ameloblasts in the *Ambn*$^{-/-}$ tooth. However, when *Ambn*$^{-/-}$ cells were plated in the presence of ameloblastin, proliferation of these cells was significantly inhibited (Fig. 7 C, right). Proliferation of MDCK cells was not affected by exogenously added ameloblastin (unpublished data). These results indicate that ameloblastin inhibits the proliferation of ameloblasts and suggest that ameloblastin is required to maintain differentiated secretory ameloblasts.

Oral tumor formation in mutant mice

We observed that mutant mice developed soft tissue tumors in the buccal vestibule of the maxilla with age (Fig. 8 A). About 19% of the homozygous mice (6 out of 32 mice) developed lesions, with the earliest occurrence at 26 wk old (Fig. 8 B). The soft tissue tumors consisted of small epithelioid cells expressing integrin α6 and enamel matrix proteins, including amelogenin, enamelin, and tuftelin (Fig. 8, C and D). The atypical epithelium surrounded focal areas of necrotic tissue with condensed matrix staining containing calcospherites at the center. There was no ameloblastin staining in either the cells or the matrix structure. Less amelogenin staining was observed compared with other matrix proteins consistent with the expression pattern in mutant teeth. RT-PCR analysis of tumor tissue revealed expression of mRNA for enamel matrix proteins including amelogenin, enamelin, and tuftelin (Fig. 8 E). These results indicate that the tumors are derived from dental epithelium. We found that only one heterozygous mouse (1 out of 48) developed a tumor. Immunostaining (unpublished data) and RT-PCR revealed that the tumor in this heterozygous mouse did not express ameloblastin but did express other enamel matrix proteins. These cells had apparently gained the ameloblastin-null phenotype that resulted in unregulated cell proliferation.

Discussion

ECM plays a critical role in tissue development and homeostasis by mediating cell growth, migration, differentiation, invasion, apoptosis, and gene expression (Damsky and Werb, 1992; Lin and Bissell, 1993). Here, we demonstrate in tooth development that ameloblastin is required for maintaining the differentiated state of ameloblasts. In *Ambn*$^{-/-}$ mice, dental epithelial cells at early stages (E18-P1) start to elongate similar to wild-type mice, but at the beginning of the secretory

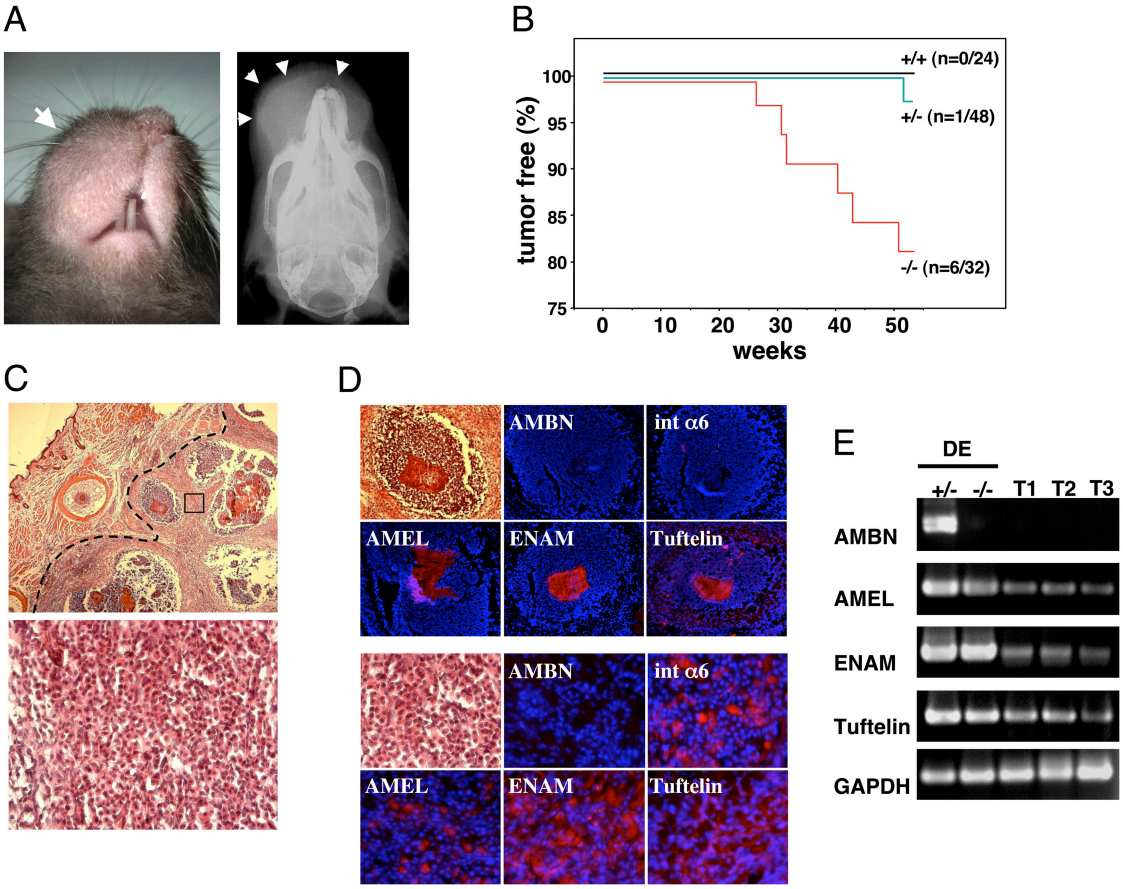

Figure 8. **Tumor formation in mutant mice.** (A) Tumor appearance in 36-wk-old homozygous ameloblastin-null mouse. Tumors were observed only on the right side of the maxillar of mutant mice. Right panel shows micro X-ray radiographs by Faxitron. Arrow and arrowheads indicate tumor. (B) Frequency of tumor formation with age. The earliest tumor was observed at 26 wk old. Only one heterozygous mouse developed a tumor. (C) Hematoxylin-eosin staining of tumor lesion of 36-wk-old mutant moue shown in A. Dotted lines indicate tumor lesions and the boxed area is enlarged at the bottom panel. (D) Immunostaining of tumor lesions. Top panel shows immunostaining of focal area and bottom panel shows surrounding cells. The focal area is stained with antibodies to enamel matrix proteins except ameloblastin, indicating accumulation of enamel matrix proteins. Cells surrounding focal areas are immunopositive for enamel matrix proteins, suggesting ameloblast origin. AMBN, ameloblastin; AMEL, amelogenin; ENAM, enamelin; int α6, integrin α6. (E) RT-PCR analysis of RNA from tumor lesions. RNA samples for lanes +/− and −/− were from dental epithelium of P7 molar of homozygous and heterozygous mice, respectively. RNA of lanes T1 and T2 was from tumor lesions of 39- and 51-wk-old homozygous mice. RNA of lane T3 was from a 51-wk-old heterozygous mouse. Note: heterozygous mouse did not express ameloblastin mRNA in the tumor but expressed mRNA for other enamel matrix proteins similar to the homozygous mice.

stage (P3 molars), cells detach from the matrix and start to lose cell polarity. In P7 mutant tooth, ameloblasts become round and smaller, completely lose polarity, resume proliferation, and form multicell layers.

In wild-type tooth, Msx2 and p75 are expressed in undifferentiated dental epithelium, but its expression is down-regulated in secretory stage ameloblasts. During mutant tooth development, expression of Msx2 and p75 is normal at the early stage, however, later when cells resume proliferation and form multicell layers, their expression is deregulated and increased, which are the cellular properties of undifferentiated dental epithelium. On the other hand, the multilayered cells of mutant tooth express enamel matrix proteins, amelogenin, tuftelin, and enamelin. This suggests that mutant dental epithelium can differentiate into enamel matrix-secreting ameloblasts. Although amelogenin is expressed in *Ambn*$^{-/-}$ ameloblasts, its expression level is significantly reduced. Msx2 was shown to inhibit promoter activity of the ameloblastin gene in DNA transfection analysis (Zhou et al., 2000). The abnormal expression of Msx2 in *Ambn*$^{-/-}$ ameloblasts is likely responsible for the down-regulation of amelogenin expression. It was also reported that Msx1 and Msx2 increase expression of cyclin D1 and inhibit cell differentiation (Hu et al., 2001). The up-regulation of Msx2 may explain the abnormal proliferation phenotype of *Ambn*$^{-/-}$ ameloblasts. These results suggest that in the absence of ameloblastin, dental epithelium can differentiate into ameloblasts but regain some early phenotypes of the undifferentiated cells.

We found that recombinant ameloblastin serves as a cell adhesion molecule. This binding activity of ameloblastin is specific to dental epithelium and not to other cell types, including MDCK epithelial cells. Although the primary culture of dental epithelium contains mixed cell types, we are able to distinguish preameloblasts and ameloblasts by immunostaining marker proteins and correlating their binding activity to ameloblastin. Using these assays, we demonstrate that ameloblasts preferentially bind to ameloblastin, but not to fibronectin and laminin 10/11. In contrast, preameloblast attachment shows the

opposite substrate specificity, i.e., preferential adhesion to fibronectin and laminin 10/11. We also demonstrate that ameloblastin inhibits proliferation of *Ambn*$^{-/-}$ ameloblasts in culture. This inhibitory activity is not observed with nonameloblast cell types, including MDCK epithelial cells, suggesting cell-type specificity. Thus, the cell binding function of ameloblastin may explain the abnormal phenotypes of ameloblasts observed in the mutant mice.

In addition to cell adhesion, ameloblastin may have another activity during enamel formation as suggested in a transgenic mouse model (Paine et al., 2003). The abnormal matrix accumulations and discontinuous calcified tissue in the mutant enamel organ do not contain typical enamel crystal structures. Ameloblastin may provide a scaffolding to organize enamel matrix protein structures to initiate crystal formation and growth. Alternatively, enamel crystal formation may require close contact of the enamel organ with newly forming dentin. In *Ambn*$^{-/-}$ mice, a thin smudgy layer coating the dentin surface is observed. This may indicate an attempt at forming enamel, yet enamel formation does not progress. Therefore, it is also conceivable that ameloblastin may play a role to sustain the progression of mineral deposition.

Deficiency of several molecules such as amelogenin, Msx2, and laminin α3 was reported to cause defects in amelogenesis. Amelogenin KO mice develop less severe enamel a defect compared with ameloblastin-KO mice (Gibson et al., 2001). In amelogenin-null tooth, ameloblasts differentiate normally and do not detach from the matrix. Amelogenin is distributed widely in the enamel matrix and is thought to play role in enamel crystallization (Fincham et al., 1999; Moradian-Oldak, 2001). Thus, ameloblastin and amelogenin appear to have a distinct function in amelogenesis (Bouwman et al., 2000; Dassule et al., 2000). In normal tooth development Msx2 is expressed in the dental epithelium and mesenchyme. Later, its expression is diminished in ameloblasts but continues in other dental epithelium such as stratum intermedium and odontoblasts (Maas and Bei, 1997). Msx2 KO tooth germs develop normally until the cap stage, however, by P1 the stratum intermedium is reduced and stratified epithelial cells accumulates in the intercuspal region and abut the ameloblast layers (Satokata et al., 2000). It seems that there is no detachment of the ameloblast layers in P9 Msx2 KO tooth. In addition, KO mice for laminin α3, a component of epithelial cell laminin 5, showed abnormal late differentiation of ameloblasts resulting in enamel hypoplasia (Ryan et al., 1999). The ameloblasts of the mutant incisors become shorter than wild-type incisors in the secretory stage, coinciding with the expression of the laminin α3 chain, and the disorganization of the reduced enamel epithelium continues throughout ameloblast differentiation. The abnormal phenotypes of ameloblastin-null mice are more severe than laminin α3-null mice.

Significant numbers of mutant mice developed tumors with age. We observed the earliest tumor formation at 26 wk old. Cells in the tumor were expressed enamel matrix proteins, suggesting that these tumors are likely derived from ameloblasts defective in ameloblastin. Consistent with this interpretation, these ameloblast-like epithelioid cells surrounded multiple focal areas consisting of enamel matrix and some calcospherites. The ameloblast-like cells likely escaped the bony crypt of the tooth before eruption and developed the tumor in the soft tissues. Human ameloblastoma is the most common odontogenic tumor (Kramer et al., 1991). It is thought to be of dental epithelial origin primarily because of histological similarity between the tumor and developing tooth (Snead et al., 1992; Abiko et al., 2001; Kumamoto et al., 2001; Yagishita et al., 2001). Toyosawa et al. (2000) reported potential mutations in the ameloblastin transcript that resulted in substitutions and a deletion of ameloblastin protein, although these mutations may not be the primary cause of ameloblastoma. More recently, the association of ameloblastin gene mutations with epithelial odontogenic tumors was reported (Perdigao et al., 2004). Although the mechanism of tumor formation in the mutant mice remains unclear, the deregulation of ameloblast differentiation due to the lack of ameloblastin is likely the primary cause of the tumor.

Materials and methods

Generation and genotyping of Ambn mutant mice

Ambn genomic clones were isolated from a mouse 129/SvEv genomic DNA library. A 10-kb genomic segment from clone 1725 containing exons 1 and 7 was used for gene targeting. A 2.5-kb XbaI–EcoRI fragment containing exons 5 and 6 was replaced with the PGK promoter-neo^r-polyA cassette from pPNT that disrupted a reading frame and created a translation termination codon. The PGK promoter-HSVtk-polyA cassette from pPNT was attached to the 3′ end of the targeting vector. The targeting vector was linearized by digestion with NotI and transfected into R1 ES cells by electroporation. ES cells were subjected to positive-negative selection and screened for homologous recombination events by genomic PCR and Southern blot analysis of genomic DNA digested with XbaI using an EcoRI fragment containing exons 7–9 as a 3′ outside probe. The wild-type and mutant alleles were detected as 4.5- and 2.3-kb fragments. Mouse chimeras were generated by injection of mutant ES cell clones into C57BL/6 blastocytes. Mutant mice were initially analyzed in the C57BL/6 × 129/SvEv mixed genetic background and later in C57BL/6 background obtained after five times backcrossed with C57BL/6. There were no phenotypic differences in these mutant mice. Animal care was given in compliance with the National Institutes of Health guidelines on this use of laboratory and experimental animals.

Radiographic and microtomography (micro-CT) analysis

8-wk-old mouse heads were dissected out and sliced sagittally into two symmetrical halves. Tooth mineral density was analyzed by a microradiographic technique using X-ray imaging with a standard setting of 90 s × 20 kV (model MX20; Faxitron X-ray Corporation). Hemimandibles from both heterozygote and homozygote mice, fixed for histological analysis (see below), were imaged in the wet state with a SkyScan-1072 X-ray microtomography system (SkyScan) operated at 80 kV.

Light microscopy of plastic-embedded teeth and SEM analyses

Some incisors fixed as below were decalcified in 4.13% EDTA, dehydrated in graded ethanol, and processed for embedding in LR white resin as described previously (Nanci et al., 1998). 1-μm-thick sections were cut with glass knives, stained with toluidine blue and examined with an Axiophot light microscope (Carl Zeiss MicroImaging, Inc.). Other calcified incisors were fractured at several sites along their length, dehydrated in ethanol, critical point dried with CO_2, and examined in a variable pressure scanning electron microscope (model JSM 5910 LV; JEOL).

Preparation of tissue sections and immunohistochemistry

E18, P1, P3, P7, and 6-wk-old mouse heads were dissected out and fixed with 4% PFA in PBS overnight at 4°C. Tissues were decalcified with 250 mM EDTA/PBS for 3 d and embedded into OCT compound (Sakura Finetechnical Co.) for frozen sectioning. Sections were cut at 8 μm on a cryostat (2800 FRIGOCUT; Leica). For 6-wk-old mouse head preparation, mice were anesthetized and fixed by perfusion with 4% PFA/PBS. The

maxilla were dissected out, fixed after overnight at 4°C in 4% PFA/PBS, decalcified with 250 mM EDTA/PBS for 1 wk, and dehydrated into xylene through a graded ethanol series and embedded in Paraplast paraffin (Oxford Laboratories). Sections were cut at 10 μm on a microtome (RM2155; Leica). For the detailed morphological analysis of molars and incisors, sections were stained with Harris hematoxylin (Sigma-Aldrich) and Eosine Y (Sigma-Aldrich). For staining of cultured cells, cells were fixed with 4% PFA/0.5% Triton X-100/PBS for 5 min and 4% PFA/PBS for 10 min.

Immunohistochemistry was performed on sections, which were incubated in 1% BSA/PBS for 1 h before incubation with primary antibody. We used antibodies directed against ameloblastin (Krebsbach et al., 1996), amelogenin (a gift from J. Simmer, University of Michigan, and M. Zeichner-David, University of Southern California, Los Angeles, CA), enamelin (a gift from J. Simmer), dentin sialoprotein (a gift from J. Simmer), tuftelin (a gift from M. Zeichner-David), PCNA (MAB424; CHEMICON International, Inc.), collagen IV (AB756; CHEMICON International, Inc.), laminin (AB2034; CHEMICON, International, Inc.), integrin α6 (GoH3; BD Biosciences), laminin γ2 (Sugiyama et al., 1995), Msx2 (sc-15396; Santa Cruz Biotechnology, Inc.), p27 (sc-528; Santa Cruz Biotechnology), and p75 (PRB-602C; Covance). Primary antibodies were detected by Cy-3 or FITC-conjugated secondary antibodies (Jackson ImmunoResearch Laboratories). Nuclear staining was performed with Hoechst dye (Sigma-Aldrich) or DAPI (Vector Laboratories). A fluorescent microscope (Axiovert 200; Carl Zeiss MicroImaging, Inc.) was used for immunofluorescent image analysis. Images were prepared using AxioVision and Photoshop (Adobe Systems, Inc.).

RNA isolation and RT-PCR

Developing molars were dissected from P3 mice. RNA was isolated using the TRIzol reagent exactly as described previously (Life Technologies). First strand cDNA was synthesized at 42°C for 90 min using Oligo(dT)$_{14}$ primer. PCR amplification was performed using primers listed in Table S1 available at http://www.jcb.org/cgi/content/full/jcb.200409077/DC1. PCR was performed with 30 cycles, 90°C for 15 min, 60°C for 30 s, and 72°C for 1 min.

Silver staining and Western blotting

Developing molars were dissected from P3 mice. The samples were suspended in 50 μl of lysis buffer (1% Triton X-100, 10 mM Tris-HCl, pH 7.4, 150 mM NaCl, 10 mM $MgCl_2$). The protein samples were fractionated by SDS-PAGE and transferred into a nylon membrane. For silver staining, gel was stained with Silver Quest (Invitrogen). The blots were incubated with antibodies, and the signals were detected with an ECL kit (Amersham Biosciences). The anti-amelogenin antibodies were raised from recombinant ameloblastin (Nanci et al., 1998). Anti-amelogenin was a gift from J. Simmer.

Expression and purification of recombinant ameloblastin

The expression vector pEF6/V5-His-Topo (Invitrogen) was used to express His-tagged ameloblastin protein (mRNA residues 1–1266). The expression plasmid was transfected into COS7 cells using Lipofectamine 2000 reagent (Invitrogen). After 2 d, transfected cells were lysed by lysis buffer (1% Triton X-100, 10 mM Tris-HCl, pH 7.4, 150 mM NaCl, 10 mM $MgCl_2$), and His-tagged recombinant protein was purified by TARON purification system (CLONTECH Laboratories, Inc.) according to the manufacturer's instructions. Purified recombinant protein was separated by SDS-PAGE and confirmed by staining with Coomassie blue and immunoblotting with anti-ameloblastin antibody.

Cell cultures and cell adhesion assay

For dental epithelial cell cultures, molars from P7 mice were dissected. Molars were treated with 0.1% collagenase/0.05% trypsin/0.5 mM EDTA for 10 min, and dental epithelium was separated from dental mesenchyme. Separated dental epithelium was treated with 0.1% collagenase/0.05% trypsin/0.5 mM EDTA for 15 min and pipetted up and down well. The dental epithelium was isolated from these molars and cultured in keratinocyte-SFM medium (GIBCO BRL) supplemented with EGF and bovine pituitary extract for 7 d to remove contaminated mesenchymal cells. Cells were then detached with 0.05% EDTA, washed with DME containing 0.1% BSA, and resuspended to a concentration of 1.0×10^5/ml and used for cell adhesion assays. Rat chondrosarcoma cells were from J.H. Kimura (Henry Ford Hospital, Detroit, MI). Mouse fibroblasts (NIH3T3), human cervix adenocarcinoma (HeLa), MDCK cells, and monkey kidney cells (COS7) were obtained from the American Type Culture Collection. Human kidney epithelium (293EBNA) was obtained from Invitrogen. These cells were cultured in DME containing 10% fetal bovine serum.

Cell adhesion assays were performed in 96-well round-bottom microtiter plates (Immulon-2HB; Dynex Technologies, Inc.). Wells were coated overnight at 4°C with 10 μg/ml recombinant ameloblastin or human fibronectin (GIBCO BRL) or human laminin 10/11 (GIBCO BRL) that were diluted with PBS and blocked with 3% BSA for 1 h at 37°C. After wash, 10^4 cells were added and incubated for 60 min at 37°C. The plates were washed with PBS three times to remove unattached cells, and attached cells were treated with 0.05% trypsin/0.5 mM EDTA and counted under a microscope. To identify the expression of integrin α6 and amelogenin in attached cells, cells were replated on cover strips. At 3 h after plating, cells were fixed with 4% PFA/PBS and followed by immunohistochemistry.

Cell proliferation assays

Dental epithelial cells were obtained from P3 and P7 molars of both heterozygous and mutant mice. 10 μg/ml recombinant ameloblastin proteins were coated on 12-well culture dishes overnight at 4°C and washed with keratinocyte-SFM medium three times. 3.0×10^4 dental epithelial cells were cultured on the dish coated with or without recombinant ameloblastin for 5 d. At 1, 3, and 5 d after plating, cells were treated with 0.05% trypsin/0.5 mM EDTA, and the cell number was counted under a microscope.

Online supplemental material

Table S1 lists primer sets used for the RT-PCR analysis in Fig. 5. Online supplemental material is available at http://www.jcb.org/cgi/content/full/jcb.200409077/DC1.

We would like to thank J. Simmer, and M. Zeichner-David for generous gifts of antibodies, H. Kleinman and M. Hoffman for comments on the manuscript, and D. Kleiner for comments on tumor histology sections. We would also like to thank S. Chowdhury for excellent technical assistance and H. Grant for editorial assistance.

This work was supported in part by grants-in-aid for Research Fellows of the Japan Society for the Promotion of Science from the Ministry of Education, Science and Culture of Japan, nos. 15689025 (to S. Fukumoto).

Submitted: 13 September 2004
Accepted: 26 October 2004

References

Abiko, Y., M. Murata, Y. Ito, T. Taira, M. Nishimura, M. Arisue, T. Inoue, M. Shimono, Y. Kuboki, and T. Kaku. 2001. Immunohistochemical localization of amelogenin in human odontogenic tumors, using a polyclonal antibody against bovine amelogenin. *Med. Electron Microsc.* 34:185–189.

Adams, J.C., and F.M. Watt. 1993. Regulation of development and differentiation by the extracellular matrix. *Development.* 117:1183–1198.

Bloch-Zupan, A., T. Leveillard, P. Gorry, J.L. Fausser, and J.V. Ruch. 1998. Expression of p21(WAF1/CIP1) during mouse odontogenesis. *Eur. J. Oral Sci.* 106(Suppl 1):104–111.

Bosshardt, D.D., and A. Nanci. 1998. Immunolocalization of epithelial and mesenchymal matrix constituents in association with inner enamel epithelial cells. *J. Histochem. Cytochem.* 46:135–142.

Bouwman, P., H. Gollner, H.P. Elsasser, G. Eckhoff, A. Karis, F. Grosveld, S. Philipsen, and G. Suske. 2000. Transcription factor Sp3 is essential for post-natal survival and late tooth development. *EMBO J.* 19:655–661.

Cerny, R., I. Slaby, L. Hammarstrom, and T. Wurtz. 1996. A novel gene expressed in rat ameloblasts codes for proteins with cell binding domains. *J. Bone Miner. Res.* 11:883–891.

Cohn, S.A. 1957. Development of the molar teeth in the albiono mouse. *Am. J. Anat.* 101:295–319.

Damsky, C.H., and Z. Werb. 1992. Signal transduction by integrin receptors for extracellular matrix: cooperative processing of extracellular information. *Curr. Opin. Cell Biol.* 4:772–781.

Dassule, H.R., P. Lewis, M. Bei, R. Maas, and A.P. McMahon. 2000. Sonic hedgehog regulates growth and morphogenesis of the tooth. *Development.* 127:4775–4785.

Fincham, A.G., J. Moradian-Oldak, and J.P. Simmer. 1999. The structural biology of the developing dental enamel matrix. *J. Struct. Biol.* 126:270–299.

Fong, C.D., I. Slaby, and L. Hammarstrom. 1996. Amelin: an enamel-related protein, transcribed in the cells of epithelial root sheath. *J. Bone Miner. Res.* 11:892–898.

Gibson, C.W., Z.A. Yuan, B. Hall, G. Longenecker, E. Chen, T. Thyagarajan, T.

Sreenath, J.T. Wright, S. Decker, R. Piddington, et al. 2001. Amelogenin-deficient mice display an amelogenesis imperfecta phenotype. *J. Biol. Chem.* 276:31871–31875.

Hu, G., H. Lee, S.M. Price, M.M. Shen, and C. Abate-Shen. 2001. Msx homeobox genes inhibit differentiation through upregulation of cyclin D1. *Development.* 128:2373–2384.

Jernvall, J., S.V. Keranen, and I. Thesleff. 2000. From the cover: evolutionary modification of development in mammalian teeth: quantifying gene expression patterns and topography. *Proc. Natl. Acad. Sci. USA.* 97:14444–14448.

Kramer, I.R.H., J.J. Pindborg, and M. Shear. 1991. Histological Typing of Odentogenic Tumours. 2nd ed. Springer-Verlag, Berlin. 12 pp.

Krebsbach, P.H., S.K. Lee, Y. Matsuki, C.A. Kozak, K.M. Yamada, and Y. Yamada. 1996. Full-length sequence, localization, and chromosomal mapping of ameloblastin. A novel tooth-specific gene. *J. Biol. Chem.* 271: 4431–4435.

Kumamoto, H., K. Kimi, and K. Ooya. 2001. Detection of cell cycle-related factors in ameloblastomas. *J. Oral Pathol. Med.* 30:309–315.

Lin, C.Q., and M.J. Bissell. 1993. Multi-faceted regulation of cell differentiation by extracellular matrix. *FASEB J.* 7:737–743.

Maas, R., and M. Bei. 1997. The genetic control of early tooth development. *Crit. Rev. Oral Biol. Med.* 8:4–39.

Mitsiadis, T.A., P. Couble, E. Dicou, B.B. Rudkin, and H. Magloire. 1993. Patterns of nerve growth factor (NGF), proNGF, and p75 NGF receptor expression in the rat incisor: comparison with expression in the molar. *Differentiation.* 54:161–175.

Moradian-Oldak, J. 2001. Amelogenins: assembly, processing and control of crystal morphology. *Matrix Biol.* 20:293–305.

Nanci, A., S. Zalzal, P. Lavoie, M. Kunikata, W. Chen, P.H. Krebsbach, Y. Yamada, L. Hammarstrom, J.P. Simmer, A.G. Fincham, et al. 1998. Comparative immunochemical analyses of the developmental expression and distribution of ameloblastin and amelogenin in rat incisors. *J. Histochem. Cytochem.* 46:911–934.

Paine, M.L., H.J. Wang, W. Luo, P.H. Krebsbach, and M.L. Snead. 2003. A transgenic animal model resembling amelogenesis imperfecta related to ameloblastin overexpression. *J. Biol. Chem.* 278:19447–19452.

Perdigao, P.F., R.S. Gomez, F.J.G.S. Pimenta, and L. De Marco. 2004. Ameloblastin gene (AMBN) mutations associated with epithelial odontogenic tumors. *Oral Oncol.* 40:841–846.

Ryan, M.C., K. Lee, Y. Miyashita, and W.G. Carter. 1999. Targeted disruption of the LAMA3 gene in mice reveals abnormalities in survival and late stage differentiation of epithelial cells. *J. Cell Biol.* 145:1309–1323.

Salmivirta, K., L.M. Sorokin, and P. Ekblom. 1997. Differential expression of laminin alpha chains during murine tooth development. *Dev. Dyn.* 210: 206–215.

Satokata, I., L. Ma, H. Ohshima, M. Bei, I. Woo, K. Nishizawa, T. Maeda, Y. Takano, M. Uchiyama, S. Heaney, et al. 2000. Msx2 deficiency in mice causes pleiotropic defects in bone growth and ectodermal organ formation. *Nat. Genet.* 24:391–395.

Simmons, D., T.T. Gu, P.H. Krebsbach, Y. Yamada, and M. MacDougall. 1998. Identification and characterization of a cDNA for mouse ameloblastin. *Connect. Tissue Res.* 39:3–12; discussion 63–67.

Smith, C.E. 1998. Cellular and chemical events during enamel maturation. *Crit. Rev. Oral Biol. Med.* 9:128–161.

Snead, M.L., W. Luo, D.D. Hsu, R.J. Melrose, E.C. Lau, and G. Stenman. 1992. Human ameloblastoma tumors express the amelogenin gene. *Oral Surg. Oral Med. Oral Pathol.* 74:64–72.

Sugiyama, S., A. Utani, S. Yamada, C.A. Kozak, and Y. Yamada. 1995. Cloning and expression of the mouse laminin gamma 2 (B2t) chain, a subunit of epithelial cell laminin. *Eur. J. Biochem.* 228:120–128.

Thesleff, I., and P. Sharpe. 1997. Signalling networks regulating dental development. *Mech. Dev.* 67:111–123.

Thesleff, I., H.J. Barrach, J.M. Foidart, A. Vaheri, R.M. Pratt, and G.R. Martin. 1981. Changes in the distribution of type IV collagen, laminin, proteoglycan, and fibronectin during mouse tooth development. *Dev. Biol.* 81:182–192.

Timpl, R. 1996. Macromolecular organization of basement membranes. *Curr. Opin. Cell Biol.* 8:618–624.

Toyosawa, S., T. Fujiwara, T. Ooshima, S. Shintani, A. Sato, Y. Ogawa, S. Sobue, and N. Ijuhin. 2000. Cloning and characterization of the human ameloblastin gene. *Gene.* 256:1–11.

Yagishita, H., Y. Taya, Y. Kanri, A. Matsuo, H. Nonaka, H. Fujita, and T. Aoba. 2001. The secretion of amelogenins is associated with the induction of enamel and dentinoid in an ameloblastic fibro-odontoma. *J. Oral Pathol. Med.* 30:499–503.

Yurchenco, P.D., and J.J. O'Rear. 1994. Basal lamina assembly. *Curr. Opin. Cell Biol.* 6:674–681.

Zhou, Y.L., Y. Lei, and M.L. Snead. 2000. Functional antagonism between Msx2 and CCAAT/enhancer-binding protein alpha in regulating the mouse amelogenin gene expression is mediated by protein-protein interaction. *J. Biol. Chem.* 275:29066–29075.